

## In-plane polarized intraband absorption in InAs/GaAs self-assembled quantum dots

S. Sauvage and P. Boucaud

*Institut d'Électronique Fondamentale, URA CNRS 22, Bâtiment 220, Université Paris-Sud, 91405 Orsay, France*

J.-M. Gérard

*France Telecom, CNET Bagneux, 196 Avenue Henri Ravera, 92225 Bagneux, France*

V. Thierry-Mieg

*Laboratoire de Microstructures et Microélectronique, UPR CNRS 20, 196 Avenue Henri Ravera, 92225 Bagneux, France*

(Received 23 February 1998; revised manuscript received 20 May 1998)

In-plane polarized photoinduced intraband absorption is reported in InAs/GaAs self-assembled quantum dots in the 90–600-meV energy range. This in-plane absorption mainly originates from bound-to-continuum transitions in the conduction and valence bands and lies in the 4–8- $\mu\text{m}$  spectral range. The continuum is constituted either by the dot quasibound states hybridized with the wetting layer subbands or by the delocalized states of the barriers. A weak in-plane polarized bound-to-bound hole transition is also observed at 11  $\mu\text{m}$ . Its in-plane absorption cross section is estimated to be around  $1.6 \times 10^{-16} \text{ cm}^2$ . The energy position of the  $p$ -polarized and in-plane polarized intraband transitions is analyzed as a function of the average quantum dot size. An experimental energy diagram of the quantum dots is presented, as deduced from the interband and intraband measurements. The existence, directions, and lengths of the intraband transition dipoles are compared to the ones deduced from the numerical resolution of the three-dimensional effective mass Schrödinger equation taking into account the flat lens-shape geometry of the dots. [S0163-1829(98)04940-6]

The three-dimensional spatial confinement in self-assembled quantum dots is expected to lead to several distinctive features concerning intraband transitions. In particular, the intraband transitions, which occur between confined states in the conduction band or in the valence band, should be polarized along different space directions. It is not the case for unidirectional confined systems such as quantum wells for which intersubband transitions are well known to be predominantly polarized, at least in the conduction band, along the  $z$  growth axis confinement direction.<sup>1</sup> Intraband transitions in quantum dots have already been reported in the literature<sup>2–5</sup> but their polarization either has not been investigated in detail or was found dominated by  $z$ -polarized transitions in the midinfrared.

This article reports on the observation of in-plane polarized intraband absorption in self-assembled InAs/GaAs quantum dots using a photoinduced infrared spectroscopy technique. The amplitudes and the energy positions of the in-plane polarized absorptions are compared to the  $z$ -polarized intraband absorptions. The temperature effect on the depopulation of the dots is used to separate the contributions from the electrons and from the holes. The effect of the dot size on these in-plane transitions is investigated. The direct observation of  $z$ -polarized and in-plane polarized transitions enables the construction of an experimental energy diagram of the dots. The energy, amplitude, and polarization of the intraband transitions are compared to the ones given by the calculation of the electronic states in a InAs quantum dot.

Two undoped samples of different distribution average size and named A1 (big dots) and A2 (small dots) have been grown by molecular beam epitaxy and extracted from the same wafer. The growth conditions, the photoluminescence

(PL) data as well as the experimental details of the infrared absorption measurement are fully described in Ref. 5, Secs. II and III. The samples are constituted by 30 InAs layers separated by 50-nm GaAs barriers. The lens-shaped InAs/GaAs dots are typically 15–25 nm wide and 2–3 nm high and their density is typically  $4 \times 10^{10} \text{ cm}^{-2}$  in each InAs layer. For photoinduced infrared measurements,<sup>6</sup> electron-hole pairs are generated using an interband optical pumping provided either by a diode laser at 824 nm or a Ti:sapphire laser tunable between 690 and 960 nm. Below the energy of the  $HH_1-E_1$  wetting layer (WL) transition at around 1.47 eV,<sup>7</sup> the carriers are directly created in the quantum dots whereas above 1.47 eV they are created in the InAs WL or the GaAs barriers and then are trapped in the dots where infrared absorption can occur. By comparison with the work presented in Ref. 5, we now take advantage of the increased population efficiency of the dots when the pump wavelength is tuned at the WL energy.<sup>7</sup> Due to an increase of the sensitivity of the experiment we have access to very weak transitions that will lead to a detailed description of the electronic structure of the dots.

Figure 1 depicts the photoinduced infrared absorption of sample A1 at 30 K and 150 K. The polarization is set either  $s$  or  $p$  as described in the inset. In the  $s$  polarization configuration, the electric field of the probe light is in the layer plane. In  $p$  polarization, the electric field has one component along the (001)  $z$  growth axis and one component of equal amplitude in the layer plane. Though the in-plane component directions of the  $s$  and  $p$  polarizations are not the same, we will not distinguish them in the following and they will be referred to as both in-plane or  $s$  polarization.

In a previous work, we analyzed the  $p$ -polarized photoinduced absorption of these InAs/GaAs quantum dots as a

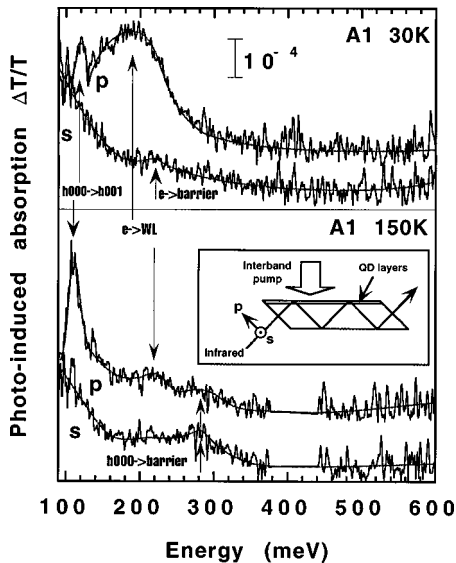


FIG. 1. Photoinduced absorption of sample A1 at 30 and 150 K in  $p$ - and  $s$ -polarizations. The interband optical pump wavelength is 824 nm and its power 40 mW on a 3 mm by 3 mm spot. Due to strong background fluctuations between 380 and 440 meV at 150 K, the irrelevant data in this energy range have been removed for clarity. The curves have been offset vertically but the relative scale is always the same and given by the vertical bar. Beyond 500 meV the signal level is zero for all curves. The smooth grey lines are guides to the eye. The inset describes the experimental configuration of the multipass waveguide geometry.

function of the temperature, the dot size, and the pump intensity and wavelength.<sup>5</sup> These results led us to assign the  $p$ -polarized infrared resonances to  $z$ -polarized intraband transitions in the dots. More specifically we attributed the narrow resonance in the  $p$  polarization at 120 meV at 30 K in Fig. 1 to the  $h000 \rightarrow h001$  bound-to-bound hole transition and the  $p$ -polarized broad band absorption around 190 meV at 30 K to a bound-to-continuum electron transition. Here  $h000$  stands for the hole ground state. The excited states are sorted according to their wave-function nodes. Following this convention,  $h001$  stands for the excited state with a node along the  $z$  direction leading to the vertically polarized  $h000 \rightarrow h001$  transition.<sup>8</sup> We showed that when the temperature is increased from 30 to 150 K, the average size of the dots that are populated increases as a result of the thermionic depopulation of the smallest dots leading to the blueshift of the  $e \rightarrow$ continuum resonance and to the slight redshift of the  $h000 \rightarrow h001$  resonance. In addition, since the electrons are less confined than the holes, they escape first out of the dot when the temperature is increased: in Fig. 1 at 150 K one can indeed observe, at around 220 meV, the reduced  $p$ -polarized absorption of the  $e \rightarrow$ continuum transition.

We will now discuss the  $s$ -polarized absorption in Fig. 1. At 30 K, apart from the free carrier absorption monotonically increasing at long wavelength, the  $s$ -polarized infrared absorption of sample A1 is composed of one small resonance maximum at 225 meV with a full width at half maximum (FWHM) of around 60 meV. Its magnitude decreases when the temperature is increased and cannot be observed beyond 60 K. The temperature dependence of the absorption amplitude mimics the one of the  $e \rightarrow$ continuum  $p$ -polarized absorption and considering its large FWHM, we attribute this

resonance to a bound-to-continuum electron transition. The large FWHM reflects the effect of the size distribution of the dots and the bound-to-continuum nature of the transition. This  $s$ -polarized  $e \rightarrow$ continuum resonance is clearly observed at slightly higher energy than the  $p$ -polarized  $e \rightarrow$ continuum absorption. As only the ground electron state of the dot is populated in the conduction band under the present experimental conditions, this suggests that these two resonances originate from two different continua. We thus attempt to assign the broadband  $p$ -polarized absorption to a transition from the electron ground state to the InAs WL subband continuum whereas we assign the weak  $s$ -polarized resonance to a transition from the ground state to the delocalized states of the GaAs barrier continuum. By WL subband continuum one means the states of the dot continuum essentially localized in the WL plane, whereas the barrier continuum stands for the states of the dot continuum three-dimensionally delocalized around the dot. The  $e \rightarrow$ WL transition is fully  $z$  polarized, indicating that the transfer of charge during the transition is along the growth axis, from the center of the dot towards the WL. The weak  $e \rightarrow$ barrier absorption may be  $z$  polarized also but it cannot be observed within the strong  $p$ -polarized signal of the  $e \rightarrow$ WL absorption. The in-plane component of this  $e \rightarrow$ barrier transition indicates the possibility of the carrier of escaping perpendicularly to the growth axis in contrast to the quantum well case where a transition in the conduction band from a bound state to the continuum is mainly  $z$  polarized.<sup>9</sup>

At 150 K, the  $s$ -polarized infrared absorption of sample A1 is composed of one resonance located at around 280 meV and with a 90-meV FWHM. Its temperature dependence is the opposite of the  $e \rightarrow$ barrier resonance: it cannot be observed at 30 K, it appears at around 90 K, and becomes stronger with temperature up to 150 K where it is maximum. The temperature dependence of its magnitude follows that of the  $h000 \rightarrow h001$  absorption, indicating that it originates from a transition from the same  $h000$  hole ground state. It is therefore attributed to a  $h000 \rightarrow$ continuum hole transition. As in the case of electrons, the question arises as to whether we should assign this hole  $s$ -polarized resonance to a transition towards the WL-like states or barrierlike continuum of states. In analogy with the electron case, and if we discard band mixing effects,<sup>10</sup> the transition of the WL would be expected to be fully  $z$  polarized. No such  $p$ -polarized absorption is observed because, the hole state being localized at the dot base, the dipole length of the transition towards the wetting layer is smaller than in the conduction band. We thus assign the  $s$ -polarized resonance at 280 meV to the transition from the  $h000$  hole ground state to the barrier continuum. This 280-meV transition energy indicates that the barrier height from the hole ground state is greater than for the electrons (225 meV) as would be expected from a heavier effective mass in the valence band.<sup>8,10</sup> One will note that the  $p$ -polarized absorption always contains one-half of the  $s$ -polarized absorption. A careful look at Fig. 1, at 150 K in  $p$  polarization, indeed shows a weak resonance at around 280 meV. It is fairly twice as small as the one in  $s$  polarization, indicating that this  $h000 \rightarrow$ barrier transition is mainly in-plane polarized.

Figure 2 illustrates the influence of the dot size on the intraband transition energies through the photoinduced absorption of sample A2 at 120 K. Sample A2 is composed of

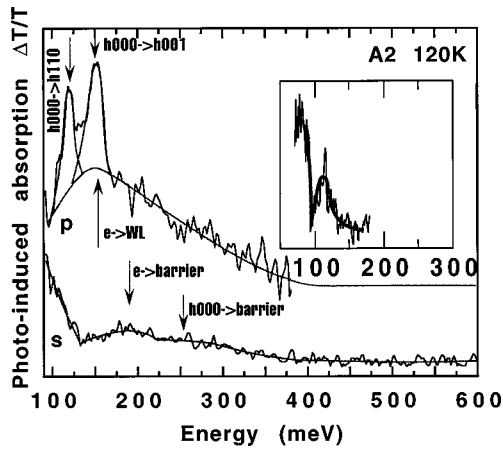


FIG. 2. Photoinduced infrared absorption of sample A2 at 120 K in  $p$  and  $s$  polarizations. Beyond 500 meV the signal level is zero for all curves. The inset depicts the in-plane polarized absorption at 120 K, which has been separately studied with a high transmission band-pass selective filter. The signal has been magnified and the free carrier absorption baseline has been removed for clarity. For the  $p$ ,  $s$ , and inset curves the conditions are (900 nm)/(40 mW), (824 nm)/(40 mW), and (845 nm)/(80 mW), respectively. The spot diameter is 3 mm. The smooth grey lines are guides to the eye.

smaller dots as compared to sample A1.<sup>5</sup> When the dot size is decreased, one expects that the energy of a bound-to-continuum transition decreases as the barrier band edge is fixed and as the WL subband edge weakly depends on the dot size.<sup>8</sup> On the contrary, the bound-to-bound transition energies are expected to blueshift for smaller dots as a consequence of the stronger confinement.<sup>8,10,11</sup>

In  $p$  polarization, sample A2 exhibits a broad resonance around 155 meV and superimposed on it two narrow resonances at 120 and 150 meV with 15 and 25 meV FWHM, respectively. A careful analysis of the infrared absorption at 120 K shows that these  $p$ -polarized resonances originate respectively from the  $e \rightarrow$ WL,  $h000 \rightarrow h110$ , and  $h000 \rightarrow h001$   $z$ -polarized transition.<sup>7</sup> It is not surprising that the  $h000 \rightarrow h110$  transition lies at lower energy than the  $h000 \rightarrow h001$  transition because the dots investigated here are flat and the confinement along the growth axis is much stronger than the confinement in the layer plane. The relatively small FWHM of the bound-to-bound transitions is a consequence of the weak dependence of the transition energies with the dot size as foreseen by various calculations in the literature.<sup>8,10,11</sup>

At 120 K, the in-plane polarized resonances of the  $e \rightarrow$ barrier and  $h000 \rightarrow$ barrier transitions are observed at around 185 and 250 meV, respectively. Again, the effective barrier height from the ground state is greater in the valence band than in the conduction band. These energies respectively correspond to a 40-meV and a 30-meV redshift as compared to sample A1.<sup>12</sup> This redshift of the intraband transitions is indeed expected from a reduction of the dot size. The stronger size effect on the electron transition is coherent with a smaller effective mass in the conduction band.

The  $h110$  hole wave function is localized near the base and at the edge of the lens-shaped dots. The dipole of the  $h000 \rightarrow h110$  transition is liable to have a component in the layer plane. The 90–180-meV energy range has thus been

selected with a high transmission filter. The inset of Fig. 2 reports the  $s$ -polarized absorption of sample A2 at 120 K. The signal has been magnified and the free-carrier baseline has been removed for clarity. We find that there is an in-plane polarized resonance, maximum at around 115 meV and with a FWHM of approximately 20 meV, close to the FWHM of  $h000 \rightarrow h001$   $z$ -polarized resonance. The low-energy signal is not yet understood and could not be further analyzed because of the detector cutoff energy. This measurement, however, shows that the  $h000 \rightarrow h110$  transition is not fully  $z$  polarized but that its dipole has a weak in-plane component. The 5-meV energy difference between the  $p$ - and  $s$ -polarized absorption is attributed to the finite resolution of the spectrum (2 meV) and a dot size dependence of the transition polarization and amplitude. The observation of this transition demonstrates that both bound-to-continuum and bound-to-bound intraband transitions of self-assembled quantum dots can be polarized in the layer plane.

The absorption cross section  $\sigma$ , for one dot layer, is the important parameter that indirectly measures the oscillator strength or the dipole length of an intraband transition. It is related to the absorption  $\alpha$  for one dot plane by  $\alpha = \sigma n$  where  $n$  is the density of the carriers populating the dots. In the present experiment, the value of  $n$  is not exactly known. One way to get it would be to seek the saturation of the absorption (as done for the  $h000 \rightarrow h001$  transition of sample B in Ref. 5). Another path is to modulation dope a sample with a known doping level. A measurement of the direct absorption in an  $n$ -doped sample of InAs/GaAs dots has led to  $\sigma_z \approx 3 \times 10^{-15} \text{ cm}^2$  for the  $e \rightarrow$ WL transition.<sup>13</sup> We will assume that it is the cross section of the  $e \rightarrow$ WL transition in samples A1 and A2. In sample A1, as the intensity of the  $e \rightarrow$ barrier absorption at 30 K is 12% of the intensity of the  $e \rightarrow$ WL  $p$ -polarized absorption recorded in the same conditions, one deduces  $\sigma_s \approx 1.8 \times 10^{-16} \text{ cm}^2$  for the in-plane polarized  $e \rightarrow$ barrier absorption. At 30 K, we assume that the density of holes contributing to the infrared absorption is the same as the density of electrons. Thus, one gets  $\sigma_z \approx 1.5 \times 10^{-15} \text{ cm}^2$  for the  $h000 \rightarrow h001$  transition because its amplitude is twice as small as the one of the  $e \rightarrow$ WL transition. At 120 K, the  $s$ -polarized  $h000 \rightarrow$ barrier absorption is 25% of the  $p$ -polarized  $h000 \rightarrow h001$  absorption. Again one gets  $\sigma_s \approx 1.9 \times 10^{-16} \text{ cm}^2$  for in-plane polarized  $h000 \rightarrow$ barrier transition. Similar amplitude comparisons give the absorption cross sections for the in-plane polarized transitions of sample A2 (summarized in Table I). The overall conclusion is that the *observed* in-plane polarized absorptions are typically one order of magnitude smaller than the  $z$ -polarized absorption. In the case of the bound-to-bound transitions, and following a quantum well approach,<sup>5</sup> dipole lengths can be deduced from the cross sections and the FWHM of the transitions. These lengths, reported in Table I, will be analyzed in the simulation part of this article. We did not attempt to deduce the dipole length for the bound-to-continuum transitions because of the mixing of inhomogeneous and bound-to-continuum broadenings.

From the direct measurement of the transition energies, one can now draw the overall energy diagram of the quantum dots in the presently investigated infrared energy range 90–600 meV. Figure 3 reports the discussed experimental

TABLE I. Absorption cross sections of the intraband transitions in samples A1 and A2 and, in the case of bound-to-bound transitions, FWHM, and dipole length.

| Transition (polarization)          | $\sigma_{A1}$ , FWHM, length                         | $\sigma_{A2}$ , FWHM, length                         |
|------------------------------------|--|--|
| $e \rightarrow$ barrier ( $s$ )    | $1.8 \times 10^{-16} \text{ cm}^2$                   | $2.5 \times 10^{-16} \text{ cm}^2$                   |
| $h000 \rightarrow h110$ ( $s$ )    | not observed   | $1.6 \times 10^{-16} \text{ cm}^2$ , 20 meV, 0.22 nm |
| $h000 \rightarrow h110$ ( $z$ )    | not observed   | $1.4 \times 10^{-15} \text{ cm}^2$ , 15 meV, 0.56 nm |
| $h000 \rightarrow h001$ ( $z$ )    | $1.5 \times 10^{-15} \text{ cm}^2$ , 20 meV, 0.70 nm | $1.4 \times 10^{-15} \text{ cm}^2$ , 25 meV, 0.65 nm |
| $h000 \rightarrow$ barrier ( $s$ ) | $1.9 \times 10^{-16} \text{ cm}^2$                   | $3 \times 10^{-16} \text{ cm}^2$                     |

transition energies of sample A1 at 150 K and sample A2 at 120 K as well as the maximum PL energy at the corresponding temperature.

As already noted, the transition energies are coherent with the nature of the carriers: considering the barrier height from the ground state to the continuum, the electron ground state is less deeply confined than the hole ground state by around 60 meV. It is the consequence of the smaller effective mass of the electrons despite the higher conduction band offset.<sup>10</sup> In the conduction band, only one bound state is observed. As will be shown below the conduction band exhibits two excited electron states lying at an energy that cannot be presently reached. More specifically the small in-plane confinement in these flat dots leads to an  $e000 \rightarrow e010$  or  $e000 \rightarrow e100$  electron transition lying below 90 meV while the other excited levels ( $e110, e001$ ) hybridize with the dot continuum. The  $h000 \rightarrow h010$  and  $h000 \rightarrow h100$  transitions are also expected to lie in the far-infrared below the detector cutoff energy. It is very probable that, for the same reason,

the  $h000 \rightarrow h110$  transition has not been seen in sample A1. From this point of view, the energy of the transitions towards states that mainly originate from the confinement in the layer plane (i.e.,  $h100, h010$ ) is much lower than the observed energy of the transition towards the  $h001$  state, which mainly originates from the confinement along the growth axis. This is consistent with the flat shape of the quantum dots.

The size dependence of the transition energies is also coherent with the effect of a stronger confinement of the carriers in the smaller dots: the bound-to-bound transitions are blueshifted and the bound-to-continuum transitions are redshifted in the smaller dots. By summing the bound-to-continuum and PL transition energies, one can get an experimental estimate of the barrier band gap: 1.61 eV for sample A1 and 1.62 eV for sample A2. Here we have not taken into account the exciton binding energy in the PL energy [typically 20 meV (Ref. 8)]. These estimates, very close to one another, are much higher than the 1.495-eV bulk GaAs band gap (at 120 K) as a result of the strain in the GaAs barriers surrounding the island. They are very close to the calculated 1.65 eV (at 4 K) strained surrounding GaAs band gap as reported in Ref. 10 for InAs/GaAs quantum dots of similar geometry thus confirming the validity of the assignment of the broadband infrared resonances.

We now compare the dipole lengths and experimental energy diagram of sample A2 (small dots) to the ones deduced from the calculation of the electronic states in one quantum dot. Various calculations in InAs/GaAs quantum dots have been published in the literature.<sup>8,10,11,15</sup> In the simulations presented here, the flat lens-shape geometry of the dots has been taken into account in order to get the theoretical dipole lengths of the intraband transitions. We solve the single-particle three-dimensional Schrödinger equation within the effective-mass approximation for the conduction band and the heavy-hole band.<sup>8</sup> Due to strain, the light-hole band lies high in energy and will not be considered.<sup>8,10</sup> The effective mass is taken diagonal in direct space.  $m_0$  standing for the bare electron mass,  $m_{xy}$  for the effective mass in the layer plane,  $m_z$  for the effective mass along the growth axis, the effective mass in the conduction band is  $m_{xy} = m_z = 0.04m_0$  in InAs and  $m_{xy} = m_z = 0.0665m_0$  in GaAs.<sup>10</sup> As underlined in Ref. 10 the electron effective mass in InAs dots is 1.7 larger than bulk InAs ( $0.023m_0$ ) as a consequence of the strain conditions. In the valence band the effective mass undergoes the effect of the strain too. Following Refs. 10 and 14 we take  $m_{xy} = 0.07m_0$  for the in-plane heavy-hole mass and  $m_z = 0.590m_0$  along the growth axis. In the GaAs regions, masses are given by their bulk values:  $m_{xy} = 0.112m_0$ ,  $m_z = 0.377m_0$ . The potential profile of one dot

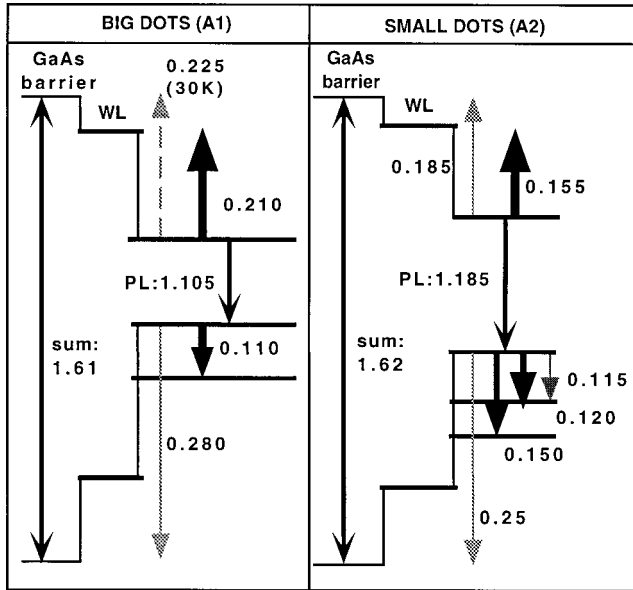


FIG. 3. Experimental energy diagram of sample A1 at 150 K and of sample A2 at 120 K as deduced from PL measurements and infrared absorption in the investigated energy range of 90–600 meV (not to scale). The black (respectively grey) arrows represent an intraband transition observed in  $p$  (respectively  $s$ ) polarization. The dotted arrow corresponds to a measurement made at 30 K. The transition energy in eV is given near each transition. The arrow thickness is a guide for the eye indicating the transition oscillator strength.

is constituted, in a GaAs matrix, by an InAs portion of a sphere 2 nm high, 20 nm in diameter lying on a 0.5-nm-thick InAs wetting layer. The overall system is embedded in a larger infinite wall box (100 nm by 100 nm by 10 nm) to limit the size of the finite difference equation and ensure null wave function conditions far from the dot. The flatness of the dot ensures nearly constant strain and constant potential in the InAs and GaAs regions: the barrier height is 600 meV in the conduction band and 450 meV in the valence band.<sup>10</sup> One will note that the barrier heights do not strongly affect bound-to-bound intraband transition energies, as in the quantum well case. Piezoelectric fields are neglected again because of the aspect ratio of the dot.<sup>15</sup> In the following, the dipole of a state means the dipole from that state to the ground state of the same band.

In the conduction band, we find that the first ( $e100$ ) and second ( $e010$ ) excited states are degenerate and lead to an  $e000 \rightarrow e010$  and an  $e000 \rightarrow e100$  transition at 76 meV with a 3.3-nm dipole length in the layer plane. Their calculated energy position confirms that we could not experimentally observe these states and indicates that it should give rise to a strong normal incident absorption. The calculated  $e110$  state, which lies 158 meV away from the ground state, is the first of a series of states located close to or in the WL continuum.  $e110$  slightly leaks in the wetting layer. This feature corresponds to the hybridization of  $e110$  with the WL states. Although  $e110$  is slightly delocalized, a dipole length of 0.15 nm along the growth axis is calculated. The direction of the dipole is coherent with the direction we experimentally observe for the  $e000 \rightarrow \text{WL}$  transition. A correct analysis of the bound-to-continuum  $e \rightarrow \text{WL}$  transition would involve all the WL states, which is not numerically manageable here. However, the 0.15-nm dipole length calculated for  $e110$  already shows that the intensity of such a bound-to-continuum absorption is not negligible.

In the valence band, the  $h000 \rightarrow h110$  transition is calculated at 108 meV with a 0.21-nm dipole length along the growth axis and the  $h000 \rightarrow h001$  transition at 201 meV with a dipole length of 0.52 nm along the same axis. The energy of  $h000 \rightarrow h110$  is very close to the energy we observe experimentally. As expected from a heavier in-plane effective mass the calculated energy is smaller than the corresponding transition in the conduction band. The  $h000 \rightarrow h001$  energy is one-third higher than the 150 meV transition energy measured experimentally indicating that the InAs effective mass  $m_z$  may be underestimated. A similar parabolic band calcu-

lation in a quantum well would have given the same trend, i.e., overestimation of the calculated energy of the highest excited states.

As in the conduction band, the dipole directions of the  $h000 \rightarrow h110$  and  $h000 \rightarrow h001$  transitions correspond to the polarization, i.e.,  $z$ , of the observed absorptions. The calculated dipole for  $h000 \rightarrow h001$  suits well the measured 0.65 nm length. However, the simulation shows that the  $h000 \rightarrow h110$  transition is weaker than  $h000 \rightarrow h001$ . This feature is less marked experimentally although the order of magnitude is reproduced. The fact that  $h110$  gets a part of the oscillator strength is not straightforward: no vertical dipole is expected for the  $h000 \rightarrow h110$  transition in a cubic dot. But the experiment and calculation demonstrate that the envelope function of the  $h110$  state, of in-plane confinement origin, is sufficiently squeezed along the growth axis for it to lead to a nonvanishing  $z$ -polarized transition with the ground state. The model also predicts that an in-plane polarized  $h000 \rightarrow h110$  transition is forbidden: it is basically the consequence of the spatial  $C_{2v}$  symmetry of the dot. However, as underlined in Ref. 10, valence-band mixing effects can lead to deviations from the  $C_{2v}$  symmetry predictions. One will note that the experimental in-plane dipole length (0.22 nm) is short: though it leads to an observable absorption, it is two orders of magnitude smaller than the 25-nm in-plane confinement length. In comparison the calculated dipole for the  $h000 \rightarrow h010$  or  $h000 \rightarrow h100$  transition, located at 51 meV, is 3.1 nm.

In conclusion, in-plane polarized infrared absorption in InAs/GaAs self-assembled quantum dots has been reported and attributed to both bound-to-bound and bound-to-continuum transitions. The influence of the average dot size has been studied and confirms the assignment of the infrared resonances. The cross section of the *observed* in-plane polarized absorptions (at an energy greater than 90 meV) are typically one order of magnitude smaller than the cross sections of the  $z$ -polarized absorptions. A detailed experimental energy diagram of the self-assembled quantum dots has been deduced from both the interband and intraband measurements. The measured dipole directions and lengths are in good overall agreement with the ones deduced from the calculation of the electronic structure based on the resolution of the Schrödinger equation in the envelope function formalism.

This work has been supported by DGA/DSP under Contract No. 97062.

<sup>1</sup>L. C. West and S. J. Eglash, Appl. Phys. Lett. **46**, 1156 (1985).

<sup>2</sup>Ch. Sikorski and U. Merkt, Phys. Rev. Lett. **62**, 2164 (1989).

<sup>3</sup>H. Drexler, D. Leonard, W. Hansen, J. P. Kotthaus, and P. M. Petroff, Phys. Rev. Lett. **73**, 2252 (1994).

<sup>4</sup>M. Fricke, A. Lorke, J. P. Kotthaus, G. Medeiros-Ribeiro, and P. M. Petroff, Europhys. Lett. **36**, 197 (1996).

<sup>5</sup>S. Sauvage, P. Boucaud, F. H. Julien, J.-M. Gérard, and J.-Y. Marzin, J. Appl. Phys. **82**, 3396 (1997).

<sup>6</sup>M. Olszackier, E. Ehrenfreund, E. Cohen, J. Bajaj, and J. Sullivan, Phys. Rev. Lett. **62**, 2997 (1989).

<sup>7</sup>S. Sauvage, P. Boucaud, J.-M. Gérard, and V. Thierry-Mieg, J. Appl. Phys. (to be published).

<sup>8</sup>M. Grundmann, O. Stier, and D. Bimberg, Phys. Rev. B **52**, 11 969 (1995).

<sup>9</sup>C. Sirtori, F. Capasso, and J. Faist, Phys. Rev. B **50**, 8663 (1994).

<sup>10</sup>M. A. Cusack, P. R. Briddon, and M. Jaros, Phys. Rev. B **54**, 2300 (1996); M. A. Cusack, P. R. Briddon, and M. Jaros, *ibid.* **56**, 4047 (1997).

<sup>11</sup>L. R. C. Fonseca, J. L. Jimenez, J. P. Leburton, and R. M. Martin, Phys. Rev. B **57**, 4017 (1998).

- <sup>12</sup>Here the  $e \rightarrow$  barrier energy shift, from sample A1 to sample A2, is underestimated because the  $e \rightarrow$  barrier transition of sample A1 has been measured at 30 K and would be blueshifted at 120 K.
- <sup>13</sup>S. Sauvage, P. Boucaud, F. H. Julien, J.-M. Gérard, and V. Thierry-Mieg, Appl. Phys. Lett. **71**, 2785 (1997).

- <sup>14</sup>L. R. Wilson, D. J. Mowbray, M. S. Skolnick, M. Morifuji, M. J. Steer, I. A. Larkin, and M. Hopkinson, Phys. Rev. B **57**, 2073 (1998).
- <sup>15</sup>Ph. Lelong and G. Bastard, Solid State Commun. **98**, 819 (1996).